The Oxygen Permeation Properties of Nanocrystalline CeO₂ Thin Films

K. S. Brinkman,[a,z] **H. Takamura,**[b,*] **H. L. Tuller,**[c,*] **and T. Iijima**[d]

[a]*Savannah River National Laboratory, Aiken, South Carolina 29808, USA*
[b]*Department of Materials Science, Graduate School of Engineering, Tohoku University, Sendai 980-8579 Japan*
[c]*Department of Materials Science and Engineering, Massachusetts Institute of Technology, Cambridge, Massachusetts 02139, USA*
[d]*Research Center for Hydrogen Industrial Use and Storage, National Institute of Advanced Industrial Science and Technology, Tsukuba, Ibaraki 305-8565, Japan*

The measurement of oxygen flux across nanocrystalline cerium oxide (CeO₂) thin films at intermediate temperature (650–800°C) is presented. Porous ceria support substrates were fabricated by sintering with carbon additions. The final dense film was deposited from an optimized sol–gel solution resulting in a mean grain size of 50 nm, which displayed oxygen flux values of up to 0.014 μmol/cm² s over the oxygen partial pressure range from air to helium gas used in the measurement at 800°C. The oxygen flux characteristics confirm mixed ionic and electronic conductivities in nanocrystalline ceria films and demonstrate the role of size dependent materials properties as a design parameter in functional membranes for oxygen separation.
© 2010 The Electrochemical Society.   [DOI: 10.1149/1.3503519] All rights reserved.

There has been significant interest in examining electrical property modification induced in nanocrystalline oxides, as compared with their conventional bulk counterparts. The ability to tailor the ionic and electronic conductivities by controlling processing and grain size is expected to deliver significant improvements in electrochemical device applications, such as fuel cell components,[1] oxygen permeation membranes,[2,3] and sensors.[4,5] Cerium oxide (CeO₂) has been a model system for these studies beginning with Chiang et al., who discovered a drastic increase in the electronic conductivity of nanocrystalline samples near atmospheric oxygen pressure where bulk cerium oxide showed exclusively ionic conductivity.[6]

This increase in the electronic conductivity was attributed to a decrease in the energy required for the reduction of nanometer size cerium oxide, as compared to coarsened bulk ceramics. These results have been confirmed in numerous reports on ceramics[7] and thin films[8,9] and are now commonly explained in the context of the "space charge model" of grain and grain boundary behavior, as discussed by Tuller,[10,11] Tschope et al.,[7] and Kim and Maier.[12] The charged defect species which are expected to accumulate at the grain boundary regions to reduce the overall system energy are charge compensated by bulk ionic and electronic defects, leading to a region of space charge which affects the material's transport properties. The width of this space charge region is related to the Debye screening length, estimated to be a few tens of nanometers.[10,11]

While the effect of decreasing grain size on electron concentration enhancement is clear, the impact of these increased defects on the transport properties such as oxygen flux and ionic conductivity is currently the topic of intense investigation. In cerium oxide, the predominant bulk defect is the positively charged oxygen vacancy which is depleted in the space charge region. A suppression of the ionic conductivity should occur if the space charge region dominates the material response, as recently observed in pure and Gd doped nanocrystalline cerium oxide ceramics.[12] However, higher doping levels of Gd, up to 30% in ultrathin cerium oxide films, where the thickness (50 nm) was comparable with the grain size (50 nm), gave recent evidence of an increase in the ionic conductivity due to the reduced contribution of perpendicular grain boundaries in contrast to that predicted from arguments based on space charge.[1] Other instances of increased ionic conductivity include measurement in a planar geometry parallel to heterojunctions in two phase systems such as BaF₂ and CaF₂, where an increase in the ionic conductivity was observed with decreasing thickness of the individual layers in a stacked structure.[13]

The result of increased electronic conductivity in nanocrystalline cerium oxide results in "mixed conductivity," including both significant electronic and ionic contributions. One of the implications of this phenomenon is the ability of the material to separate oxygen from air using only the chemical potential gradient of oxygen as the driving force, without the application of an external bias field as is required in oxygen "pumps" often based on zirconia and ceria materials.[14]

Since normal sintering temperatures of 1500°C result in large micrometer size grains in the cerium oxide system, the fabrication of nanocrystalline ceramics has been problematic. A recent publication demonstrates the use of spark plasma sintering techniques for producing dense nanocrystalline ceramics.[15] Thin films fabricated by sol–gel,[16] sputtering,[17,18] spray pyroloysis,[8] Pulsed Laser Deposition (PLD),[19] and CVD (Ref. [20]) have been common routes to achieving dense nanocrystalline cerium oxide. However, although numerous reports of the electrical conductivity of thin film ceria exist in the literature, the authors are not aware of any reports on the oxygen permeation properties of nanocrystalline cerium oxide ceramics or thin films. This is due to the difficulty of preparing a dense thin film on a suitable porous substrate. Recently, a sol–gel method was used to deposit Gd doped cerium oxide and CoFe₂O₄ spinel composite thin films on porous ceramic substrates, of the same composition, for oxygen permeation measurement.[2]

The focus of this manuscript is on the intermediate temperature oxygen permeation characteristics of nanocrystalline ceria thin films prepared by a sol–gel method. Porous support substrates of cerium oxide were prepared with densities of 80% by the pyrolysis of carbon additions, as described in Ref. [2] for Gd doped cerium substrates. A sputtered "blocking layer" of cerium oxide was deposited on the surface of polished cerium substrates in order to reduce the solution's leakage into the porous substrate. Finally, sol–gel solutions were spin coated onto the substrate, followed by pyrolysis and annealing in a box furnace. The resulting oxygen flux of 0.014 μmol/cm² s at 800°C under an oxygen gradient in ceria is an evidence of mixed conductivity, as discussed below.

Experimental

Sample preparation and characterization.— The porous cerium oxide substrates were prepared by ball milling cerium oxide (High Purity Chemical Co., Japan) with 7 wt % carbon powder (NICA-BEADS, Nippon Carbon Co., Ltd., Japan) in ethanol for 24 h. After drying and sieving, the powder was mixed with a binder and uniaxi-

ally pressed into pellets of 16 mm diameter with a force of 20 kN and sintered at 1500°C for 6 h in air. Sintered ceramic samples had relative densities of 70% (30% porous) with pore sizes of 1 to 3 μm and a physical gas flux greater than 2 μmol/cm² s, deemed sufficient to provide air to the dense ceria membrane for the permeation measurements in this study. The fabrication of pure cerium oxide substrates in this work is analogous to the preparation of porous Gd doped ceria substrates by Kagomiya.[2]

A significant problem with the porous ceramic substrates reported in the work of Kagomiya[2] was the subsequent leakage of the sol–gel solution used for film fabrication into the substrate during spin coating. In the present work, this problem was overcome by sputter depositing a layer of cerium oxide onto the polished porous substrate surface in order to inhibit sol–gel solution leakage into the porous substrate. Sputtering was performed on a JEOL, Tokyo, Japan (JEC-SP360M) system at 200 W and 0.5 Pa of Ar gas at room temperature using a cerium oxide target.

The final step in sample preparation was the chemical solution deposition of a ceria sol onto the porous substrate and blocking layer. The solution processing of cerium oxide poses another obstacle for thin film fabrication as ceria has a tendency for agglomeration and precipitation in solution, thus limiting the maximum achievable concentration.[21] Concentrations exceeding 0.2 M prepared with Ce acetate and acetylacetonate (acac) solutions in acetic acid/water (ratio 2:1) were found to be unstable. In the present study, an optimized sol–gel process was obtained using cerium III acetylacetonate (Aldrich, USA, chemicals) in an acetic acid/water solvent. The ceria acac precursor was mixed with 30 mL of acetic acid and 15 mL of deionized water, followed by heating to 120°C and held under reflux conditions for 1 h, resulting in a clear yellow colored solution. The solution was deposited by spin coating onto the porous cerium oxide substrates with a predeposited cerium oxide buffer layer at 3000 rpm for 30 s, followed by drying for 3 min at 100°C and pyrolysis for 3 min at 350°C. This procedure was repeated ten times before heat-treatment in a box furnace to 800°C for 30 min in air. The process was repeated to obtain multilayer films consisting of 60 sol–gel layers. The final film thickness was nominally 500 nm. Thin film development of cerium oxide by sol–gel and sputtering methods were performed on Pt/Si substrates with rapid thermal annealing to 800°C for 10 min in air following film deposition.

The crystal structure of the ceramics and thin films were examined by X-ray diffraction (Philips, XRD, Tokyo, Japan, X-pert), and the microstructure was examined by SEM (JEOL). The mean grain size was determined by an average of 50 grains using the software package ImageJ.[22]

Oxygen flux measurement.— Oxygen flux measurements were performed by placing the sample between two quartz tubes using a glass ring (melting point 620°C) for gas sealing and a metal spacer with a diameter of 5 mm to control the area of gas flux. Air at 1 atm was supplied to the bottom of the porous substrate (feed side), while flowing He (20 sccm) was supplied to the permeate side (film surface). The gas concentrations of O_2 and N_2 were measured on the permeate side using a gas chromatograph (GC323; GL Sciences Co. Ltd., Tokyo, Japan). The leakage of oxygen was calculated by measuring the volume of N_2 gas from air on the permeate side. The oxygen permeation flux was corrected using the total measured oxygen on the permeate side minus the physical leakage of oxygen. In the present case, leakage of air was not completely eliminated, most likely due to possible cracks or damage to the thin film surface during the glass sealing process and/or remaining low levels of porosity in the film. However, the physical leakage of oxygen comprised less than 10% of the total concentration of oxygen measured on the permeate side at 800°C. The leakage was constant with temperature (as measured by the N_2 concentration), while the oxygen concentration increased due to increased oxygen transport through the membrane. The oxygen concentration measured on the permeate side at 800°C was 0.012% corresponding to a oxygen partial pres-

sure $P(O_2)$ of 10^{-4} atm. The concentrations of oxygen and nitrogen measured were well within the calibrated range for the GC, and a repetition of these results on numerous samples confirmed that the majority of oxygen detected was in fact due to oxygen transport through the cerium oxide film.

The measurement of the oxygen flux through the sample can be formally described by the Wagner equation, Eq. 1[23]

$$J(O_2) = -\frac{RT}{16F^2L} \int_{\ln P(O_2)'}^{\ln P(O_2)''} \frac{\sigma_i \sigma_e}{\sigma_i + \sigma_e} d \ln P(O_2) \qquad [1]$$

where σ_i and σ_e are the ionic and electronic conductivities, $P(O_2)'$ and $P(O_2)''$ are the oxygen partial pressure on the feed and permeate sides, respectively, T is the temperature in kelvin, R is the gas constant, F is the Faraday constant, and L is the membrane thickness.

Surface effects have the potential to be the rate determining step and can be described by a modification of Eq. 1 to include a characteristic length, below which a decrease in the thickness does not lead to an increase in measured oxygen flux.[24] In ceria–ferrite based composite ceramic membranes with micrometer size grains fabricated by conventional ceramic processing, significant limitations due to surface exchange kinetics were observed at membrane thicknesses less than $L = 0.5$ mm under a large oxygen partial pressure gradient from Ar-5%H_2 to air. Under a less severe oxygen partial pressure gradient from He to air used in this report, as well as the much reduced oxygen fluxes obtained in this study, the characteristic length would be smaller than this value and the oxygen flux should be controlled by bulk diffusion. In general, the characteristic length depends on the ratio of surface exchange to bulk diffusion of the ionic species and has been reported to range from hundreds of nanometers to thousands of micrometer, depending on the material system, microstructure, morphology, and measurement conditions.[25-27] Recent data on the thickness dependence of nanocrystalline ceria–ferrite thin film membranes on porous substrates similar to films fabricated in the present study have demonstrated that the oxygen flux is inversely proportional to the membrane thickness, even with thicknesses in the range of 2 μm.[28]

Using the assumption in nanograin ceria[6] that $\sigma_e > \sigma_i$, Eq. 1 may be rearranged to give an estimate of the ionic conductivity from the measured oxygen flux[29]

$$\sigma_i = \frac{J(O_2)}{\ln\left(\frac{P(O_2)'}{P(O_2)''}\right)} \frac{16F^2L}{RT} \qquad [2]$$

where σ_i is the ionic conductivity (S/m) assumed $P(O_2)$ independent, $J(O_2)$ is the oxygen permeation flux (mol/m² s), R is the gas constant (8 1314 J/mol K), T is the temperature (kelvin), F is the Faraday constant (96 485 C/mol), L the thickness of the membrane (500 nm) and $P(O_2)'$ and $P(O_2)''$ are the oxygen partial pressures on the feed and permeate sides. The concentration of gas at the permeate sides $P(O_2)''$ in the argon sweep gas was determined by the GC and was subsequently used as the oxygen partial pressure "driving force" for ionic conduction.

Results and Discussion

Initial experiments indicated that sputtered layers of 1 μm in thickness on porous cerium oxide substrates were ineffective in preventing air leakage during oxygen permeation measurements. Therefore, dense layers of cerium oxide were deposited by a sol–gel method on the surface of the sputtered cerium oxide. This composite structure had the advantage of reduced solution leakage into the substrate with a sputtered layer, as compared to the substrate itself. Since films of cerium oxide were required from both sol–gel and sputtering methods for the experiments in this report, the films were characterized separately on Pt/Si substrates. Figures 1a and b display the X-ray and SEM determined microstructure for ceria films fabricated by sol–gel and sputtering methods onto Pt/Si substrates. The X-ray diffraction spectrum of the sol–gel film shows peaks from
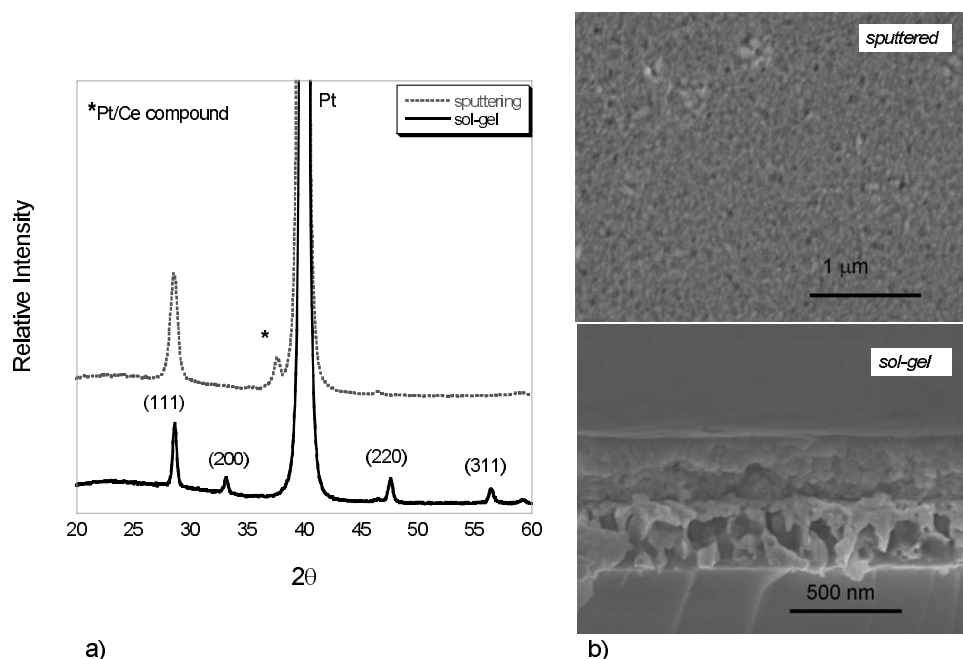
Figure 1. (a) X-ray diffraction of cerium oxide thin films deposited on Pt/Si substrates by sol–gel and sputtering methods. (b) SEM determined microstructure.

ceria and the Pt substrate, while sputtered films show the presence of a PtCe compound, most likely due to the increased energies of the sputtering process. The microstructure of the films was dense with nanometer size grains.

Figure 2 displays the X-ray spectra of the Fig. 2a bare porous cerium oxide substrate and the Fig. 2b substrate with both sputtered and sol–gel cerium oxide films. The X-ray broadening observed is indicative of the reduced grain size of cerium oxide thin films, as compared to the ceramic substrate. The microstructure of the film/ceramic substrate is shown in Fig. 3. In Fig. 3a we see a expanded view of the substrate with micrometer size pores due to carbon burnout during sintering. The sputtered cerium oxide buffer layer can also be seen to grow in a columnar fashion up from the substrate/film interface. A close-up of the dense sol–gel derived cerium oxide film and the sputtered cerium oxide buffer layer is shown in Fig. 3b, clearly showing the columnar nature of the sputtered

layer with a mean column diameter of 90 nm and the dense sol–gel layer with a mean grain size of 50 nm and a nominal film thickness of 500 nm.

The oxygen flux characteristics for the nanocrystalline cerium oxide film on a porous substrate are presented in Fig. 4a. At low temperatures near 654°C it is seen that the oxygen concentration in the permeate side from oxygen flux through the membrane is approximately equal to the amount of oxygen in air that passed through as leakage. As the temperature increased to 804°C, the oxygen flux due to oxygen transport through the membrane increased an order of magnitude to 0.014 μmol/cm^2, while the amount of oxygen due to leakage remained constant, accounting for less than 10% of

Figure 3. SEM determined microstructure. (a) Large view of porous substrate, 1 μm sputtered cerium oxide layer and dense sol–gel cerium oxide layer (b) Close-up of dense sol–gel cerium and sputtered cerium oxide buffer layer.
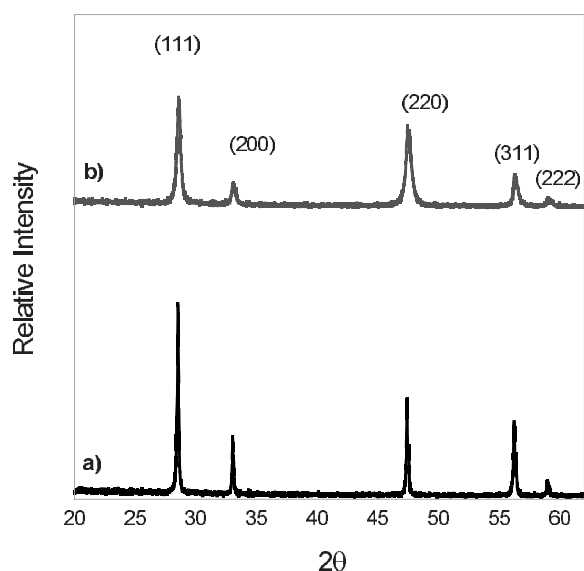

Figure 2. X-ray diffraction spectra of (a) porous cerium oxide substrate and (b) substrate after sputtered and sol–gel cerium oxide thin film deposition.
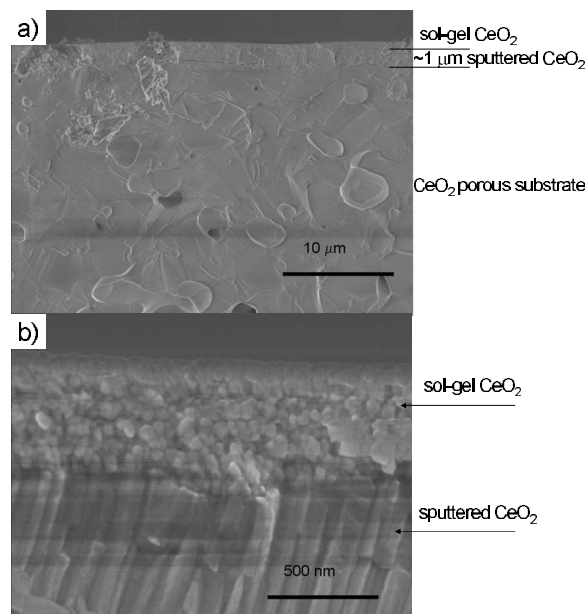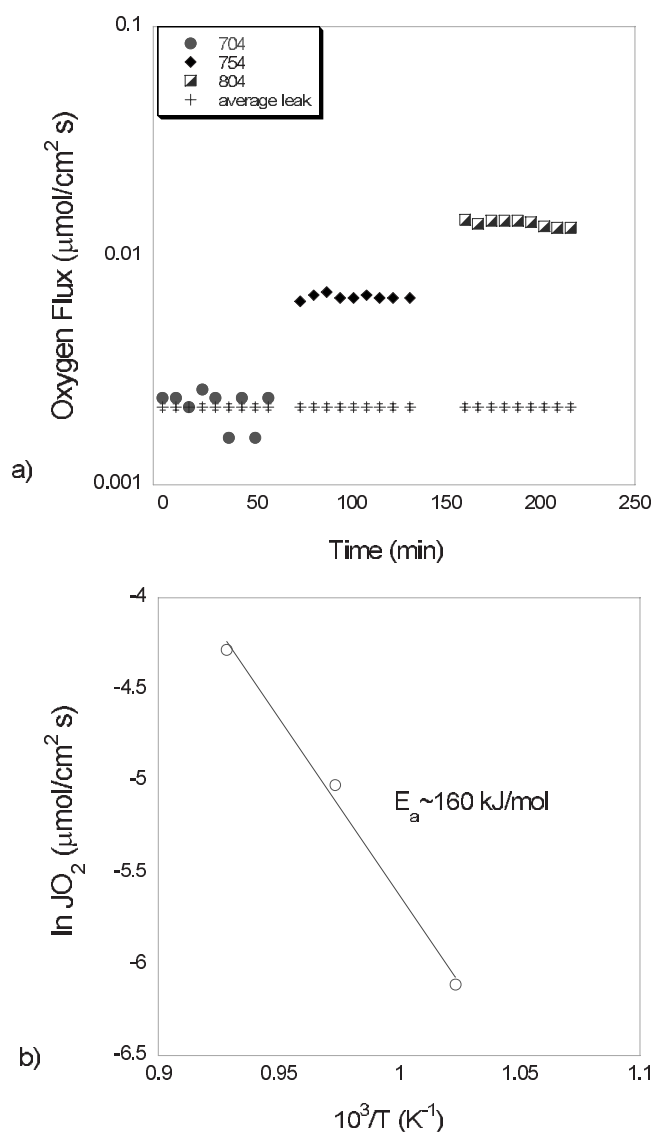
Figure 4. (a) Oxygen flux [μmol/cm^2 s] as a function of time at temperatures of 654, 704, and 804°C. Included is the mean oxygen flux due to air leakage as determined from nitrogen concentration in the permeate stream. (b) Activation energy of oxygen flux $E_a = 160$ kJ/mol.

Table I. Ionic conductivity at 800°C of nanocrystalline cerium oxide in this work estimated from oxygen flux data using Eq. 2 compared with bulk and nanocrystalline forms of cerium oxide from literature. An ionic conductivity activation energy of 153 kJ/mol for nanocrystalline cerium oxide was used to extrapolate data from Ref. 38 and 33 to 800°C.

Sample	σ_i (S/cm)	Reference
CeO$_2$ 50 nm grain size	6×10^{-7}	This work (Eq. 2)
CeO$_2$ 50 nm grain size	1×10^{-5}	38
CeO$_2$ 50 nm grain size	8×10^{-3}	33
CeO$_2$ bulk form	5×10^{-4}	34
Ce$_{0.8}$Gd$_{0.2}$O$_2$ bulk form	1×10^{-1}	34

which is very close to the value of 160 kJ/mol reported in this study.[33] When including space charge effects, the activation energy for the oxygen ion conductivity becomes[33]

$$E_v^\perp = E_{v\infty} + 2e\left(\Delta\phi(0) + \frac{1}{T}\frac{\delta\Delta\phi(0)}{\delta 1/T}\right) \qquad [3]$$

Here, E_v corresponds to the activation energy for vacancies traveling perpendicular to the grain boundaries, $E_{v\infty}$ is the activation energy of the ionic conductivity in the neutral region of the grain, and $\phi(0)$ is the space charge barrier potential. Using values of 0.3 V for $\phi(0)$ and 0.1 V for $(1/T)\delta\phi(0)/(\delta 1/T)$, the large reported values for the activation energy for ionic conduction in nanocrystalline ceria films can be understood.[33]

The ionic conductivity of the films fabricated in this study calculated from the modified Wagner relation equation 1 were on the order of 10^{-7} S/cm, a value significantly less than bulk ceramics. The ionic conductivity in undoped ceramics is on the order of 10^{-4} S/cm, while highly aliovalent doped cerium oxide can approach 10^{-1} S/cm at 800°C.[34] The trend of a decrease in ionic conductivity with decreasing grain size is consistent with space charge effects induced adjacent to positively charged grain boundary cores, resulting in the depletion of oxygen vacancies. Table I summarizes the ionic conductivity values for bulk and nanocrystalline ceria from literature reports. Assuming an activation energy of 153 kJ/mol to include space charge effects for the ionic conductivity of 50 nm ceria, the reported conductivity values vary from 10^{-3} to 10^{-5} S/cm at 800°C, as compared to the 10^{-7} S/cm estimate from the present work. It is noted that estimates of ionic conductivity using Eq. 1 and 2 do not take into account surface effects. Estimates of the oxygen surface exchange rate J_{ex} (μmol/cm^2 s) from the surface exchange coefficient k (cm/s), of nanocrystalline ceria thin films,[35] normalized to the molar concentration, c_i (mol/cm^3), of oxygen ions at equilibrium, give a value of 0.2 μmol/cm^2 s, an order of magnitude above the oxygen flux (0.014 μmol/cm^2 s) measured in the current experiment,[36] suggesting that surface effects are not limiting in the present case. In addition, if the flux was in the surface exchange limited regime, the temperature dependence (activation energy) of the oxygen flux should be different than that outlined above for oxygen ionic conduction in nanocrystalline ceria including space charge effects. Lane and Kilner have experimentally determined values of 3.3 eV or 337 kJ/mol (Ref. 37) for the surface exchange activation energy in ceria over twice the observed activation energy for oxygen flux observed in this study. Lastly, a study of thickness dependence down to the micrometer level for nanocrystalline films of a similar ceria-ferrite system, indicating bulk diffusion control, points to the major role that bulk diffusion must play in the present system.[28]

In addition to bulk diffusion and surface effects, material preparation routes are known to play a major role in impurity content and conductivity levels, especially at elevated temperatures. The ceria
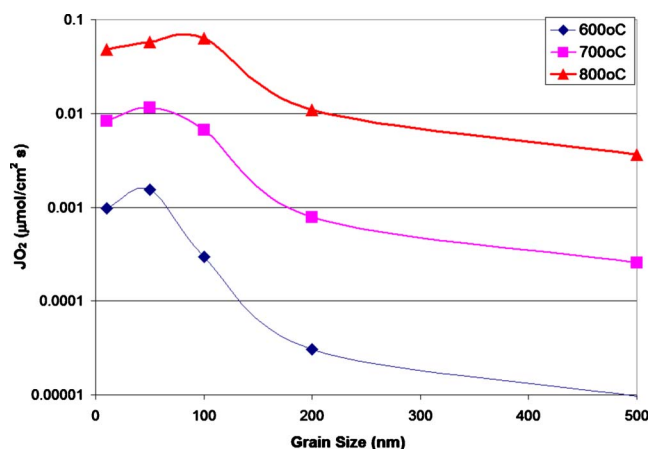
the total measured oxygen concentration on the permeate side at 804°C. Figure 4b shows the activation energy for oxygen flux through the thin ceria membrane, determined from the logarithm of oxygen flux versus reciprocal temperature to be approximately 160 kJ/mol.

Given that nanocrystalline ceria is expected to conduct predominantly by electrons, the oxygen flux, according to Eq. 1 and 2, should be limited by the minority ionic conductivity. At first glance, the relatively large activation energy measured for the oxygen flux of 160 kJ/mol would appear to be more consistent with the electronic conductivity. For example, Suzuki et al. reported an energy of activation for electronic conductivity (140 kJ/mol) in 30 nm grain size CeO$_2$ thin films.[9] On the other hand, the migration energy of oxygen vacancies in the bulk has been reported in the literature to be much lower and to range from 67.5 (Ref. 30) to 86.8 (Ref. 31) to 96.5 kJ/mol.[32] However, this ignores the impact of space charge induced depletion of oxygen vacancies in the vicinity of the grain boundaries. Under these conditions, Litzelman and Tuller recently reported that the oxygen ion conductivity in nanocrystalline CeO$_2$ thin films is characterized by the activation energy of 153 kJ/mol,

Figure 5. (Color online) Oxygen flux [μmol/cm² s] as a function of grain size and temperature calculated from the Wagner relation equation 1 with size-dependent data from Ref. 38.

films fabricated in this study were made from a wet solution chemistry method that is less clean than physical vapor deposition routes and could have produced unexpected donor dopant impurities which are known to reduce the ionic conductivity by further suppressing the oxygen vacancy concentration. Therefore, the oxygen permeation values reported in this study could potentially be enhanced with an increase in the ionic conductivity to levels near 10^{-5}–10^{-3} S/cm with the concomitant elevated electronic conductivity expected in nanocrystalline ceria.

Figure 5 displays predictions of the oxygen flux versus grain size and temperature using literature data from Tschope[38] and Eq. 1 for a 500 nm thick film in the absence of surface limitations. The conductivities were assumed to be independent of oxygen partial pressure over the range from 0.21 to 10^{-5} atm $P(O_2)$. The temperature dependence of the conductivities was calculated using an ionic activation energy of 97 kJ/mol and an electronic activation energy of 222 kJ/mol for large grain size material down to 100 nm. Grain sizes below 50 nm utilized an ionic activation energy of 153 kJ/mol and an electronic activation energy of 125 kJ/mol. The maximum of predicted oxygen flux between 50 and 100 nm grain size corresponds to the maximum ambipolar conductivity, resulting in flux values near 0.06 μmol/cm² s at 800°C compared to experimentally determined flux of 0.014 μmol/cm² s presented in this work. Figure 6 shows the impact of oxygen partial pressure driving force on the

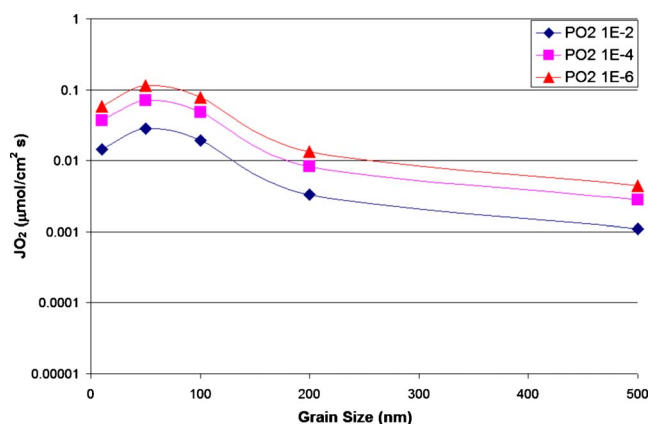predicted permeation of nanocrystalline CeO₂ membranes at 800°C. The flux predictions were calculated given a constant feed side partial pressure of 0.21 atm, while the downstream concentration of oxygen was varied between 10^{-2} and 10^{-6}, resulting in an oxygen flux varying from 0.028 to 0.114 μmol/cm². In the absence of surface limitations, it was observed that the oxygen flux could exceed 1 μmol/cm² s for films with ionic conductivities on the order of 10^{-3} S/cm, approaching the flux target of oxygen/air separation membranes by using solely CeO₂ as a single material system. The functionality of electronic conduction is provided by the nanocrystalline materials structure as opposed to second phase additions such as noble metal additions commonly added in dual phase membranes. Future work is warranted which focuses on the thickness dependence of oxygen flux in nanocrystalline ceria films from the micrometer to the nanometer regime as well as the grain size dependent surface exchange parameters in conditions relevant to membrane separations.

Conclusion

Nanocrystalline CeO₂ cerium oxide thin films were fabricated on porous cerium oxide substrates using both sol–gel and sputtering deposition techniques. The samples showed a measurable oxygen flux of 0.014 μmol/cm² s at 800°C confirming mixed ionic and electronic conductivities and demonstrating the feasibility of utilizing nanocrystalline CeO₂ as an oxygen separation membrane with grain size as a design parameter. Calculations of the oxygen permeation using the size and temperature dependence of ionic and electronic conductivities from literature predict a maximum oxygen flux near 50 nm grain size corresponding to the maximum ambipolar conductivity and the nominal grain size presented in this work.

Acknowledgments

References

1. H. Huang, T. Gur, Y. Saito, and F. Prinz, *Appl. Phys. Lett.*, **89**, 143107 (2006).
2. I. Kagomiya, Y. Iijima, H. Kakuta, and H. Takamura, *Electrochem. Solid-State Lett.*, **8**, A70 (2005).
3. I. Kagomiya, T. Iijima, and H. Takamura, *J. Membr. Sci.*, **286**, 180 (2006).
4. P. Jasinski, T. Suzuki, and H. Anderson, *Sens. Actuators B*, **96**, 73 (2003).
5. A. Tschope, J. Ying, and H. Tuller, *Sens. Actuators B*, **31**, 111 (1996).
6. Y.-M. Chiang, E. Lavik, I. Kosacki, H. Tuller, and J. Ying, *Appl. Phys. Lett.*, **69**, 185 (1996).
7. A. Tschope, E. Sommer, and R. Birringer, *Solid State Ionics*, **139**, 255 (2001).
8. J. Rupp and L. Gauckler, *Solid State Ionics*, **177**, 2513 (2006).
9. T. Suzuki, I. Kosacki, and H. Anderson, *Solid State Ionics*, **151**, 111 (2002).
10. H. L. Tuller, *Solid State Ionics*, **131**, 143 (2000).
11. H. L. Tuller, S. J. Litzelman, and W. Jung, *Phys. Chem. Chem. Phys.*, **11**, 3023 (2009).
12. S. Kim and J. Maier, *J. Am. Ceram. Soc.*, **24**, 1919 (2004).
13. N. Sata, K. Eberman, K. Eberl, and J. Maier, *Nature (London)*, **408**, 946 (2000).
14. D. Meixner, D. Brengel, B. Henderson, J. Abrardo, M. Wilson, D. Taylor, and R. Cutler, *J. Electrochem. Soc.*, **149**, D132 (2002).
15. U. Anselmi-Tamburini, F. Maglia, G. Chiodelli, A. Tacca, G. Spinolo, P. Riello, S. Bucella, and Z. Munir, *Adv. Funct. Mater.*, **16**, 2363 (2006).
16. N. Rane, H. Zou, G. Buelna, and J. Lin, *J. Membr. Sci.*, **256**, 89 (2005).
17. L. Kim, J. Kim, D. Jung, C. Park, C. ang, and Y. Roh, *Thin Solid Films*, **360**, 154 (2000).
18. G. Chiodelli, L. Malavasi, V. Massarotti, P. Mustarelli, and E. Quartarone, *Solid State Ionics*, **176**, 1505 (2005).
19. J. Rupp, A. Infortuna, and L. Gauckler, *Acta Mater.*, **54**, 1721 (2006).
20. S. Suh, J. Guan, L. Miinea, J. Lehn, and D. Hoffman, *Chem. Mater.*, **16**, 1667 (2004).
21. H. Zou, Y. Lin, N. Rane, and T. He, *Ind. Eng. Chem. Res.*, **43**, 3019 (2004).

Figure 6. (Color online) Oxygen flux [μmol/cm² s] at 800°C as a function of grain size and oxygen partial pressure on the permeate side varying from 10^{-2} to 10^{-6} atm calculated from the Wagner relation equation 1 with size-dependent data from Ref. 38.

22. W. S. Rasband, ImageJ, National Institutes of Health, Bethesda, http://rsb.info.nih.gov/ij/, 1997–2004, last accessed June 2009.
23. C. Wagner, *Z. Phys. Chem. Abt. B*, **21**, 25 (1993).
24. H. Takamura, K. Okumura, Y. Koshino, A. Kamegawa, and M. Okada, *J. Electroceram.*, **13**, 613 (2004).
25. H. J. M. Bouwmeester, H. Kruidhof, and A. J. Burggraaf, *Solid State Ionics*, **72**, 185 (1994).
26. H. W. Brinkman, J. Meijerink, K. J. de Vries, and A. J. Burggraaf, *J. Am. Ceram. Soc.*, **16**, 587 (1996).
27. Y. S. Lin, L. G. J. de Haart, K. J. de Vries, and A. J. Burggraaf, *J. Electrochem. Soc.*, **137**, 3960 (1990).
28. K. Brinkman, T. Iijima, and H. Takamura, *Mater. Res. Soc. Symp. Proc.*, **1126**, 1126 (2009).
29. Note that if σ_e is included and assumed PO$_2$ independent Eq. 2 becomes: $\sigma_i\sigma_e/(\sigma_i + \sigma_e) = [J(O_2)]/[ln(P(O_2)'/P(O_2)'')](16F^2L/RT)$. With σ_e at 800°C of 1.5 × 10^{-5} S/cm, the estimated σ_i is 6.4 × 10^{-7} S/cm as compared to 6.0 × 10^{-7} S/cm using Eq. 2.
30. S. Kim and J. Maier, *J. Electrochem. Soc.*, **149**, J73 (2002).
31. D. Y. Wang, D. S. Park, J. Griffith, and A. S. Nowick, *Solid State Ionics*, **2**, 95 (1981).
32. S. Kim, J. Fleig, and J. Maier, in *Ionic and Mixed Conducting Ceramics IV*, T. S. Ramamarayanan, W. L. Worrell, and M. Mogensen, Editors, PV 2001-16, p. 208, The Electrochemical Society Proceedings, Pennington, NJ (2001).
33. S. J. Litzelman and H. L. Tuller, *Solid State Ionics*, **180**, 1190 (2009).
34. H. Inaba and H. Tagawa, *Solid State Ionics*, **83**, 1 (1996).
35. A. Karthikeyan and S. Ramanathan, *Appl. Phys. Lett.*, **92**, 243109 (2008).
36. (i) k at 800°C taken as 3 × 10^{-5} cm/s, (ii) $c_i \sim \delta/V_m$ is 6.34 × 10^{-3} mol/cm^3, where δ is oxygen nonstoichiometry 0.15 and V$_m$ is molar volume (23.85 cm^3/mol for CeO$_{1.85}$), (iii) j$_{ex}$ = k*c_i = 2.2 × 10^{-7} mol/cm^2 s.
37. J. A. Lane and J. A. Kilner, *Solid State Ionics*, **136–137**, 927 (2000).
38. A. Tschope and R. Birringer, *J. Electroceram.*, **7**, 169 (2001).